

On the stability of the Neptune Trojans

R. Dvorak,¹[★] R. Schwarz,² Á. Süli² and T. Kotoulas³[★]

¹*Institute for Astronomy, University of Vienna, Türkenschanzstr. 17, A-1180 Wien, Austria*

²*Department of Astronomy, Eötvös University, H-1117 Budapest, Pázmány Péter stny. 1/A, Hungary*

³*Department of Physics, University of Thessaloniki, GR-541 24 Thessaloniki, Greece*

Accepted 2007 September 13. Received 2007 September 10; in original form 2007 July 18

ABSTRACT

The area of stable motion for fictitious Trojan asteroids around Neptune’s equilateral equilibrium points is investigated with respect to the size of the regions and their shape, subject to the inclination of the asteroid’s orbit.

For this task, we used the results of extensive numerical integrations of orbits for a fine grid in initial conditions around the points L_4 and L_5 and analysed the stability of the individual orbits. Our basic dynamical model was the outer Solar system (Jupiter, Saturn, Uranus and Neptune) but for comparison reasons also simpler ones were tested. We integrated in our models the equations of motion for some 5×10^5 orbits of fictitious Trojans in the vicinity of the stable equilibrium points up to 10^9 yr. According to the three-dimensional model, the initial inclination of the asteroids’ orbit was also varied in the range $0^\circ < i < 60^\circ$. Using on one side a fine grid of initial conditions, the semimajor axis versus perihelion of the fictitious object and, on the other side, the proper eccentricity e_p versus the libration width D_f , we compiled stability maps separately for L_4 and L_5 . In addition, we computed the escape-times of the individual objects and plotted the number of escapers per time-interval of 5×10^6 yr for different initial inclinations. Finally, integrations of the equations of motion in different dynamical models shed light on the reason of the asymmetry of the stability behaviour of orbits close to the two equilateral equilibrium points of Neptune.

For low-inclined Trojan orbits, the stability area around L_4 and L_5 disappeared after some 10^8 yr, and for larger inclinations of the Trojans the stability area survived for the time-interval of integration of 10^9 yr. The largest stable regions exist for Neptune Trojans with $20^\circ < i < 50^\circ$. The somewhat interesting asymmetry in the size and the shape of the preceding and following Lagrange points, which exist for Neptune Trojans, was confirmed, and was found to be caused mostly by the couple Saturn–Uranus.

Key words: methods: N -body simulations – celestial mechanics – Solar system: general.

1 INTRODUCTION

The first discovery of a Jupiter Trojan in 1906 (Achilles by Max Wolf in Heidelberg) showed that the equilateral equilibrium points in a simplified dynamical model, Sun–planet–massless body, is not only of hypothetical interest. Ever since many Trojan asteroids of Jupiter have been found and now we have knowledge of several thousands of objects with the same period as Jupiter. Investigations up to now showed a symmetry of these two stable equilibrium points only in the restricted three-body problem but not in the realistic dynamical model of the outer Solar system (OSS) consisting of Jupiter, Saturn, Uranus and Neptune like in, for example, Dvorak & Schwarz (2005), Freistetter (2006) and Schwarz, Gyergovits & Dvorak (2004).

In 2001, the first Neptune Trojan 2001 QR 322 was discovered by the Lowell Observatory’s Deep Ecliptic Survey team (Buie, Wasserman and Millis) librating around L_4 . Three more co-orbiting asteroids of Neptune were then reported to be discovered by Sheppard & Trujillo (2006), namely 2004 UP10, 2005 TN53 and 2005 TO74 (see also in Table 1). Finally, last year one more asteroid was found (2006 RJ 103) by the SDSS Collaboration. Immediate verification of the stability of their orbits with the aid of numerical integrations showed their stability over time-scales up to the age of the Solar system (see e.g. Marzari et al. 2003). All of them are close to the point L_4 and have orbits with low inclinations ($i < 10^\circ$) with the exception of TN53 with $i = 25^\circ$. These discoveries led to the assumption that there may be many more Trojans of Neptune than that of Jupiter (see e.g. Chiang & Lithwick 2005). On the contrary, it seems that Saturn and Uranus do not have this kind of companions along their orbits. In a special investigation recently Zhou & Sun

[★]E-mail: dvorak@astro.univie.ac.at

Table 1. Orbital elements of the five Neptune Trojans; for more details see Minor planet centre, <http://cfa-www.harvard.edu/iau/mpc.html>

Name	a (au)	Eccentricity	i (°)
2001 QR322	30.190	0.029	1.3
2004 UP10	30.099	0.025	1.4
2005 TN53	30.070	0.062	25.0
2005 TO74	30.078	0.051	5.3
2006 RJ103	29.973	0.028	8.2

(2007) tried to understand the large-inclination TN53 compared to the other ones. They concluded, with Thommes, Duncan & Levison (1999), that this is due to fast migration of Neptune inwards during 10^6 yr where a few bodies could be captured into orbits with large inclinations.

There exist numerical investigations of fictitious Trojans of the outer planets by Holman & Wisdom (1993) where via numerical integration (up to 2×10^7 yr) they established stability regions around the Lagrangian points of the gas giants in the framework of the OSS. They found that the region around L_4 and L_5 is symmetric with respect to the planet with the exception of Neptune. In a more recent study, Nesvorný & Dones (2002) integrated fictitious Trojans for Saturn, Uranus and Neptune up to the age of the Solar system and computed the fraction of surviving bodies in the framework of the OSS. They found that Saturn's Trojans are leaving the region around L_4 rather quickly, namely within several 10^5 yr and out of more than 200 Trojans only 1 per cent survived for the whole integration time. They found very similar results for Uranus, with the exception that the loss at the beginning of the integration (during the first million years) is relatively small, and then the depletion goes rather rapid such that at the end again only 1 per cent of the more than 200 Trojans at the beginning survived.

The picture was completely different for the Neptune Trojans: half of the initial bodies (100 also with inclinations up to 25°) close to L_4 survived over the 4.5 billion years of integration. This is quite well visible in the respective fig. 10 of the publication by Nesvorný & Dones cited above.

In our research, we concentrated on the extension of the stable regions around both Lagrange points of Neptune. The main goals of this study were the following: (i) to establish stability regions around the equilateral equilibrium points of Neptune and how the size depends on the inclinations of the orbit of the Trojan; and (ii) to understand the reason for the asymmetric structure of the regions around L_4 and L_5 found by the former mentioned study of Holman & Wisdom (1993).

From analytical and semi-analytical methods, we know how these regions look like and how different in size they are in the elliptic restricted three-body problem (ER3BP). Interesting results using Nekoroshev estimates have been derived, for example, for the Jupiter Trojans in the circular problem by Simó (1989) and by Celletti & Giorgilli (1991) who found only a very narrow region around the equilibrium points to stay stable for the age of the Solar system. Progress has been made by Giorgilli & Skokos (1997) who established a more realistic estimate for this region. Using a symplectic method, Efthymiopoulos (2005) achieved an ever better estimate with about 30 per cent of the Trojans in a region around Jupiter's equilibrium points stable for 10^{10} yr. More recently, Efthymiopoulos & Sándor (2005) could improve this estimate with a new symplectic mapping in the plane circular problem by calculating a resonant

Birkhoff normal form so that this percentage increases to almost 50 per cent of the known Jupiter Trojans. In continuation of this work, Lhotka, Efthymiopoulos & Dvorak (in preparation) constructed a mapping where they also introduced the ellipticity of the planets' orbit and established regions of effective stability times for Jupiter, Saturn, Uranus and also for Neptune. This is still a rather modest model because the perturbations of the other large planets are not taken into account. The extension of this analytical work seems possible in what concerns the secular changes in the perihelion of the planet for which the Lagrange points are studied. Unfortunately, to take into account the inclination – an important parameter for the stability regions (see our results) – seems, at least for the moment, too complicated for providing Nekoroshev estimates.

2 THE MODEL AND THE METHODS

As pointed out in the preceding section, the analytical results cannot yet give enough information for the problem in question. Therefore, we need results of long-term integrations of the orbits of fictitious test bodies in the vicinity of the equilateral equilibrium points. For Jupiter, we have many studies explaining in all details the role of three-body resonances and secular resonances inside the 1:1 mean motion resonance (e.g. Robutel, Gabern & Jorba 2005) and Saturn is known to have no stable regions for Trojans. For the integration of the equations of motion in our study, we used different methods which we used as complementary:

- (i) the MERCURY6 package of Chambers (1999); and
- (ii) the Lie-integration method (Hanslmeier & Dvorak 1984; Lichtenegger 1984).

The basic dynamical model for the numerical integrations was the Solar system with the Sun and the planets Jupiter, Saturn, Uranus and Neptune. To understand the asymmetry of the region around L_4 and L_5 for the Neptune Trojans, we also used simpler dynamical models to be able to identify the planet which is causing it. Consequently, the following eight dynamical models were used.

- (i) *M1*. The OSS.
- (ii) *M2*. Jupiter, Saturn and Neptune.
- (iii) *M3*. Uranus and Neptune.
- (iv) *M4*. The ER3BP with Neptune alone.
- (v) *M5*. Jupiter and Neptune.
- (vi) *M6*. Saturn and Neptune.
- (vii) *M7*. Jupiter, Uranus and Neptune.
- (viii) *M8*. Saturn, Uranus and Neptune.

Although the usage of chaos indicators is very important (like the Relative Lyapunov Indicators and the Fast Lyapunov Indicators or directly the Lyapunov Characteristic Indicator) for this research, the direct check of the action like variable eccentricity of the fictitious Trojans turned out to be a very good tool concerning the determination of the size of the stable regions. As a stability definition in our research, we used two different criteria: for most of the plots we determined the maximum eccentricity achieved during the integration of an orbit; and only for the plots of the escape-time (Fig. 7), we used the penetration of the asteroid into the Hill's sphere of a planet.

One important point is the choice of initial conditions: first, studies have been undertaken as the ones by the former mentioned investigations by Holman & Wisdom: there, for a certain grid of initial conditions the stability character was established via results of integrations of the equations of motion for 20 Myr. The initial

orbits of the fictitious Trojans were almost circular; the semimajor axes were varied between 29.5 and 30.7 au; for the longitude, all values between $0^\circ < \lambda < 360^\circ$ were chosen. We later decided to use proper elements for the initial conditions, which seem to be the more appropriate choice for this kind of research of massless bodies (see the next section).

3 THE PROPER ELEMENTS AND RESULTS FOR DIFFERENT INCLINATIONS

Usually, one refers to the proper elements for asteroids to characterize their orbits. There exists a very complete data set for proper elements for all numbered asteroids in the main belt and also for the Trojans computed by Milani (see <http://unicorn.eis.uva.es/cgi-bin/neodys/neoibo>). Let us briefly recall the definition of proper elements.

Érdi (1988) defined the first term of the long periodic variations in the expansion of the semimajor axis a and the relative mean longitude $\lambda - \lambda'$ for a Trojan asteroid in the following way (where $'$ refers to the elements of the planet):

$$a - a' = d_f \sin \theta + O(d_f)^2,$$

$$\sigma = \lambda - \lambda' = \frac{\pm \pi}{3} + D_f \cos \theta + O(D_f)^2, \quad (1)$$

where d_f (in au) is the amplitude of libration in the semimajor axis which relates to the amplitude of libration D_f (in radians) of the critical argument σ via

$$d_f = \sqrt{3\mu a'} D_f \sim 0.3741 D_f. \quad (2)$$

As done in former studies for the Jupiter Trojans (Tsiganis et al. 2005), an orbit in the plane σ versus $a - a'$ is topologically equivalent to a cycle where the centre is close to the Lagrange point itself (located at $\pm\pi$). The angle θ is measured from this point and circulates while the critical argument librates $\pm\pi/3 \pm D_f$. We set the initial conditions such that $\sigma = \pi/3$ and $a = a' + d_f$. Furthermore, we set the longitude of the pericentre of the Trojan $\tilde{\omega} = \tilde{\omega}' + \pi/3$ and the proper eccentricity $e = e' + e_f$. Finally, the longitude of the node was set equal to the one of Neptune and the proper inclination was simply set to $i = i' + i_f$. This choice means that the mean anomaly M of every fictitious object was set to the one of Neptune.

According to the test computations, the integration time was set to 10^8 yr for 1681 orbits (the grid of 41×41) for fictitious aster-

oids for different inclinations of the orbits in the vicinity of both Lagrange points. Normally, one assumes a complete symmetry between both equilibrium points, which is in fact not true for the region of the Jupiter Trojans. There exist no stability regions for Saturn and Uranus Trojans for time-scales which are of interest from the point of view of cosmogony. The results of the preceding section show in fact a significant difference for Neptune Trojans which we could confirm with additional computations with respect to the proper elements. We equally distributed the initial conditions $0 < e_p < 0.4$ and $D < 60^\circ$ and did our simulations for different proper inclinations for the fictitious ‘Trojan cloud’ with $0^\circ < i_p < 60^\circ$ with a step of $\Delta i_p = 5^\circ$.

The respective results for the planar problem $i_p = 0^\circ$ did not show a difference of major importance: only some orbits survived for e_p close to 0; this is already true for $i_p = 5^\circ$. In the following, we will discuss the results in detail.

(i) $i_p = 10^\circ$ (Fig. 1). Here, one can see that only for almost circular initial conditions some objects survive for the whole integration time; the upper limit for D for L_4 is around 20° , and for L_5 up to 50° ; some of the orbits stay stable.

(ii) $i_p = 20^\circ$ (Fig. 2). Both regions are significantly larger and one finds also stable orbits for eccentricities up to $e_p = 0.1$. The extension in D is almost similar to the former one.

(iii) $i_p = 30^\circ$ (Fig. 3). A somewhat different picture shows the results for the leading and the preceding Lagrange points for this relatively large inclination. The L_4 Trojans have quite a similar behaviour to that for the inclination of $i_p = 20^\circ$. The L_5 Trojans have maximum stability for $20^\circ < D < 40^\circ$ up to a proper eccentricity $e_p < 0.2$. This behaviour means that there is a strong asymmetry with respect to the semimajor axis.

(iv) $i_p = 40^\circ$ (Fig. 4). The trend, as shown in the preceding graph, continues in principle: the stable region close to L_5 is significantly larger than that close to L_4 . In addition, the latter region diminished strongly with respect to D , whereas the L_5 region is as extended as for the inclination $i_p = 30^\circ$.

(v) $i_p = 50^\circ$ (Fig. 5). The stability region for L_4 disappeared almost completely; the L_5 region shrank towards $15^\circ < D < 35^\circ$ and extends up to $e_p = 0.15$.

For larger proper inclinations ($i_p = 60^\circ$) around L_4 , there are no orbits which survive the 10^8 yr integration. For the L_5 objects, only

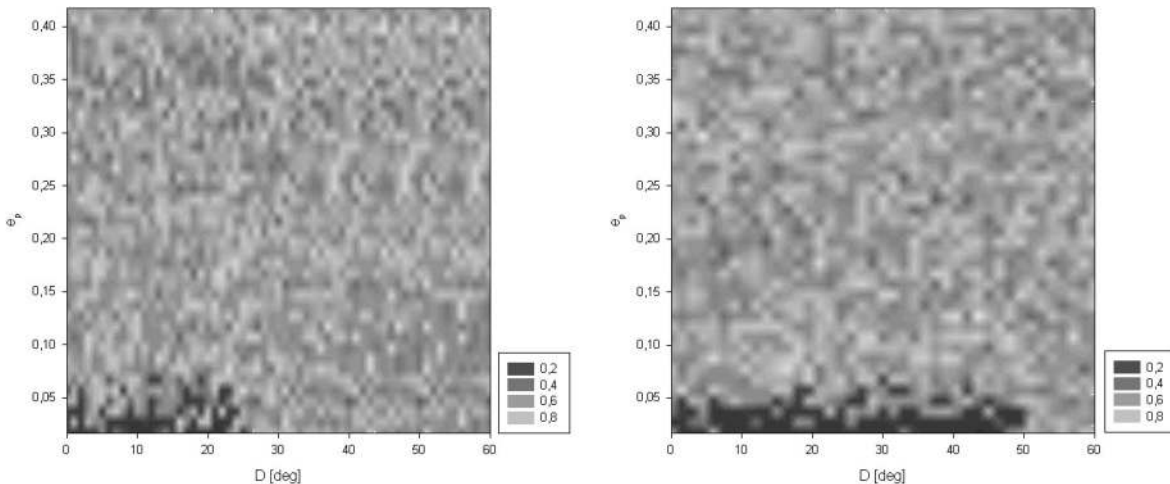


Figure 1. Stability regions around Neptune’s equilibrium points in the model of the OSS for $i_p = 10^\circ$: L_4 Trojans: left-hand side graph; L_5 Trojans: right-hand side graph. The colours are according to the maximum value of the eccentricity; dark regions represent stable orbits with an eccentricity $e < 0.2$.

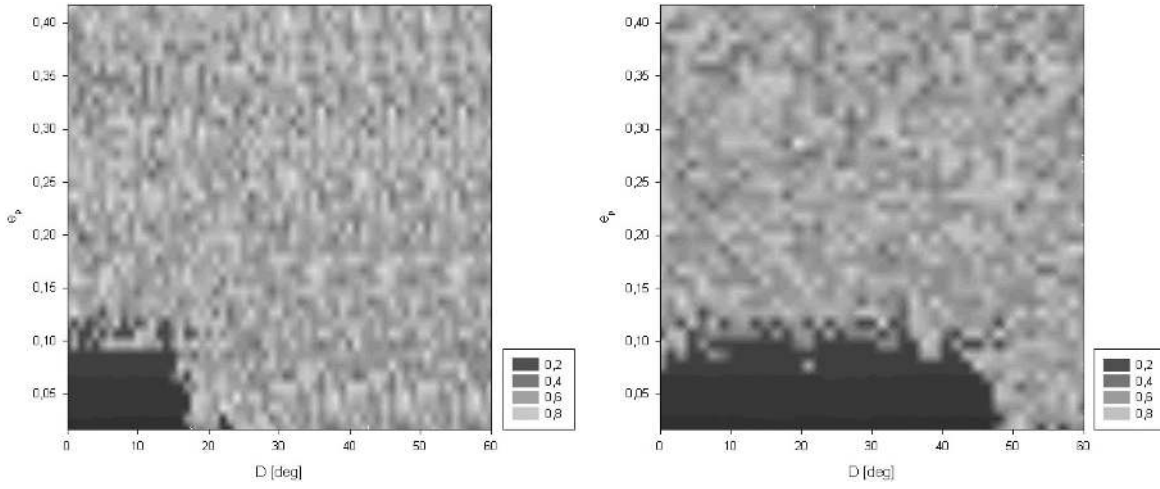


Figure 2. The same as Fig. 1 but for $i_p = 20^\circ$.

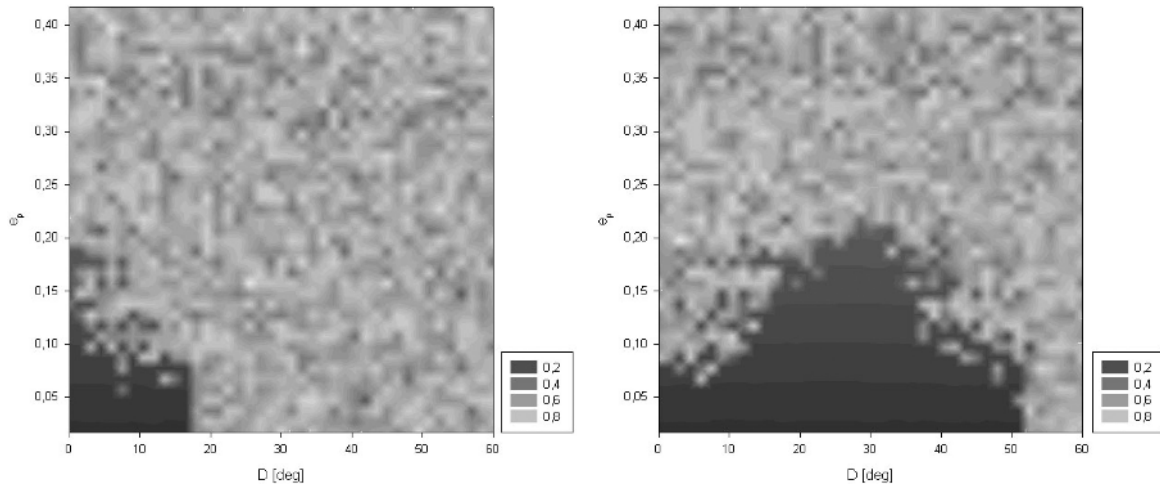


Figure 3. The same as Fig. 1 but for $i_p = 30^\circ$.

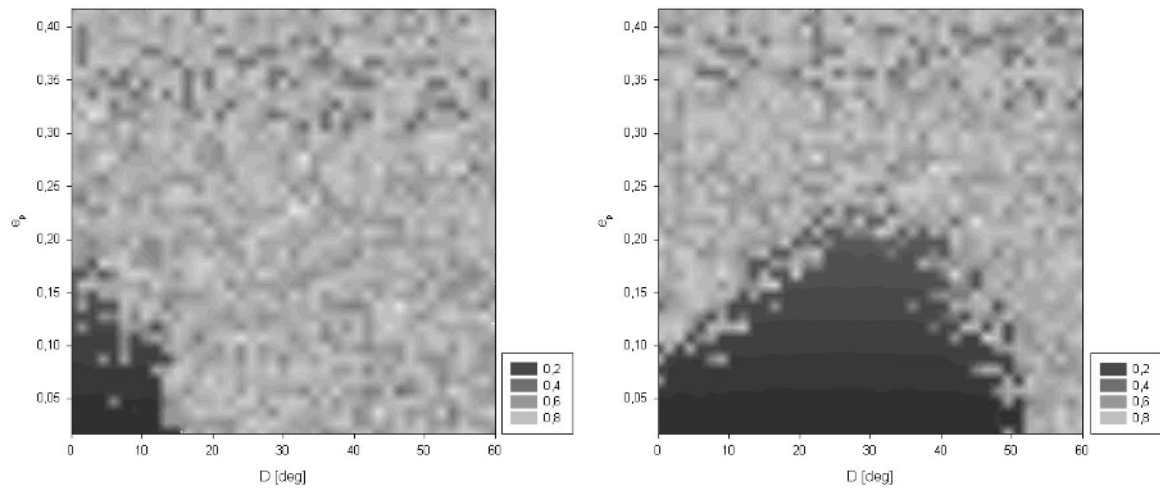


Figure 4. The same as Fig. 1 but for $i_p = 40^\circ$.

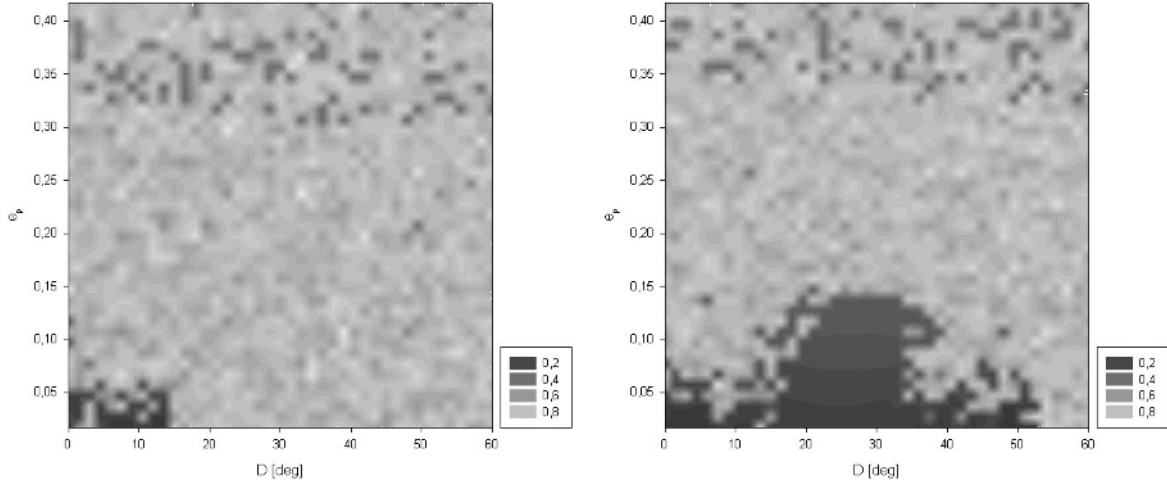


Figure 5. The same as Fig. 1 but for $i_p = 50^\circ$.

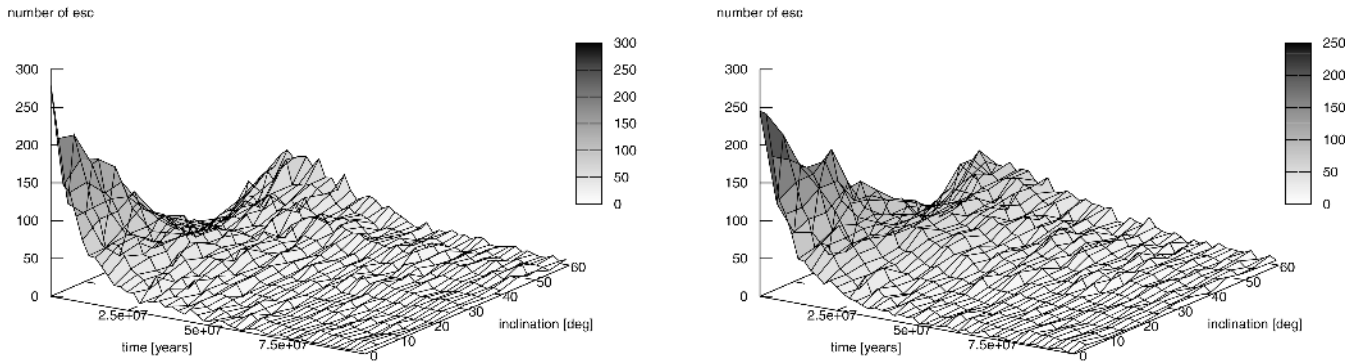


Figure 6. Escape-times for 1681 fictitious objects around the Lagrangian equilibrium points for Neptune for different proper inclinations; L_4 Trojans: left-hand side graph; L_5 Trojans: right-hand side graph.

a connected region of 20 orbits (out of 1681) is stable for $15^\circ < D < 35^\circ$ and $e_p < 0.05$.

4 DISTRIBUTION OF THE ESCAPE-TIMES

To be able to compare the different escape-times for the L_4 and L_5 Trojans, we plotted the results of the 10^8 yr integration for different initial proper inclinations (i_p). Fig. 6 shows that most of the L_4 Trojans escape within the first 10 million years; then there is more or less an exponential decrease up to the end of the integration.

For $i_p = 10^\circ$, there is almost no difference between the two equilibrium points concerning the number of escaping bodies and the escape-times. This has already been discovered on the proper element stability maps e_p versus D for the stable region (Fig. 1). For $i_p = 20^\circ$, it is evident that more bodies escape within the first 10^7 yr, whereas most of the L_5 Trojans escape within 2×10^7 yr. With $i_p = 30^\circ$, the L_4 Trojans escape within 3×10^7 yr but the number of the escaping Trojans around the following Lagrange point is significantly lower. For $i_p = 40^\circ$, both equilibrium points seem to be relatively stable compared to the other inclinations for the first 10^7 yr and then most of fictitious Trojans escape within the next 3×10^7 yr. Globally, the distribution of the escape-times concerning objects with $30^\circ < i_p < 40^\circ$ looks quite similar. For $i_p = 40^\circ$, the quantitative behaviour is again different for the two equilibrium points: for L_4 there is a maximum of escaping orbits between $10^7 <$

$T_{\text{escape}} < 2 \times 10^7$ yr; on the contrary, the escaping L_5 Trojans have a broad maximum between $10^7 < T_{\text{escape}} < 4 \times 10^7$ yr.¹

5 ON THE ASYMMETRY OF THE STABLE REGIONS AROUND L_4 AND L_5

As described already in the Introduction section, there seems to be a strong asymmetry of the stable regions around Neptune's equilateral equilibrium points when we make our computations in the realistic model with all large planets (M1). This asymmetry is quite well visible already in Fig. 7 for 10 million year integrations for the planar problem. For comparison reasons, we show also the region in this model after 10^8 yr (Fig. 8) where one sees that the stability areas around the equilibrium points are not connected regions any more. In fact, they disappear completely after 10^9 yr integration time.

In addition to this, we show as example for this asymmetry which survives for long-term integrations up to 1 Gyr, the results for $i_p = 30^\circ$ are shown in Fig. 9. Whereas the preceding point is enclosed by a stable region with L_4 well in its centre, the region around L_5 is again shifted towards the larger semimajor axis and also distorted

¹ The escape-time T_{escape} of an object from the area around the equilibrium points was defined when the 'Trojan' entered the Hill's sphere of a planet.

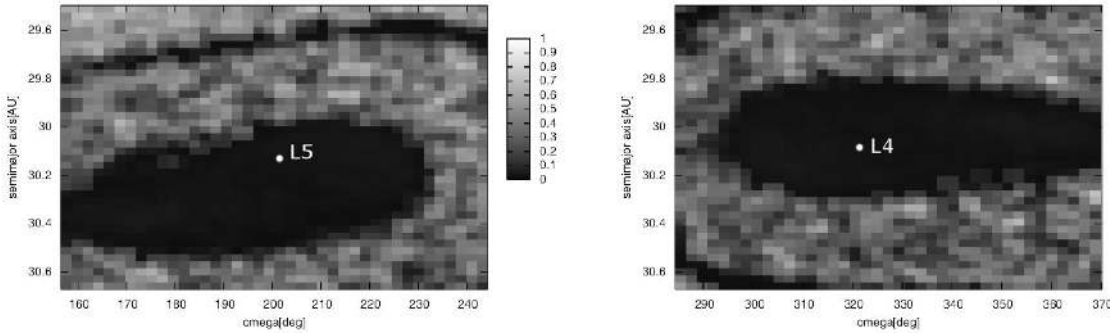


Figure 7. Stability regions around the Neptune equilateral equilibrium points L_5 (left-hand panel) and L_4 in the dynamical model of the OSS after 10^7 yr. The colour stands for the maximum eccentricity achieved during the integration; black means $e < 0.2$, etc. The shift to the larger semimajor axis for the point L_5 is well visible.

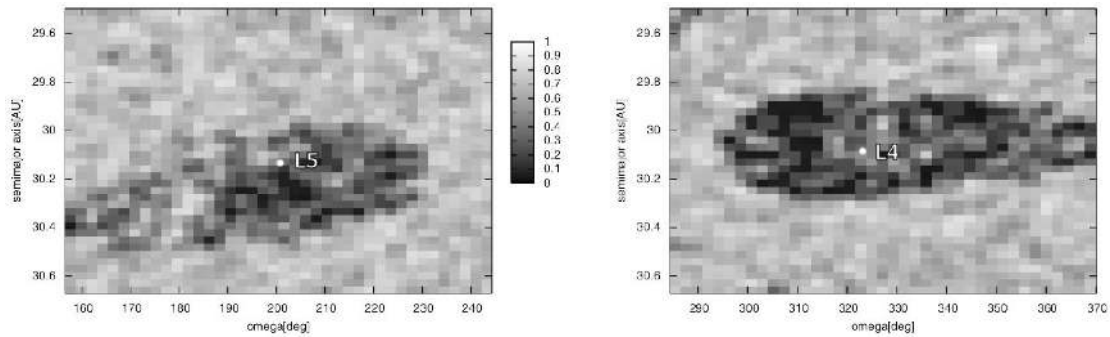


Figure 8. Stability regions around the Neptune equilateral equilibrium points L_5 (left-hand panel) and L_4 in the dynamical model of the OSS for the time-scale of 10^8 yr. The shift to the larger semimajor axis for the point L_5 is still visible as in Fig. 7.

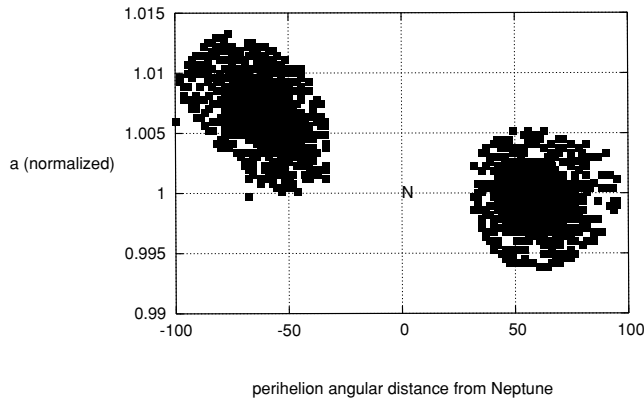


Figure 9. The asymmetry of the L_4 and the L_5 equilibrium points for the inclination $i = 30^\circ$; L_4 and L_5 are located at $a = 1$ and $\pm 60^\circ$. The results are for an integration of 10^9 yr.

to an egg-shaped area inclined 45° with the equilibrium point L_5 at the lower end (with the smallest initial semimajor axis). This difference for the two equilibrium points appears for all stable regions independent of the inclination (as mentioned above for $15^\circ < i < 50^\circ$).

Also in the respective figures above (Figs 1–5), where we plotted the stable orbits with respect to the initial e_p versus D_f , this asymmetry is well visible. In the Trojan area around Jupiter’s Lagrange points, there is no evident asymmetry with respect to the shape of the stability region, although the number of the L_4 (!) Trojans turned out to be larger than the L_5 Trojans (the ratio is 5:3). Saturn’s Trojans – as already mentioned – escape quickly (some million years); Uranus’

Trojans also escape within some 10^8 yr from the region around the equilibrium points. To unveil the reason for the specific dynamical behaviour of Neptune Trojans, we did computation in the different models described in Section 2. To compare them, we have chosen for the semimajor axis of the Trojans $29.3 \leq a \leq 30.7$ au and for the perihelion a strip of 80° around the location of the two equilibrium points. To stay within reasonable computer-time, we chose a grid of 21×21 initial conditions and integrated for different inclinations of the test bodies up to 100 Myr. We show and discuss only the results for $i = 0^\circ$ as an example for the other computations which have quite the same qualitative behaviour.

For the models M2–M7 no asymmetry at all is present. This is different for M8 (Fig. 10): the middle of the stable L_4 region is located at Neptune’s normalized semimajor axis 1 (right-hand side graph), but for the L_5 area this is the lower boundary of the stable region (left-hand side graph). In addition, the stable area is significantly smaller than that for the other models. It should be stressed that this model M8 is without Jupiter!

6 CONCLUSIONS

Discussing the results, it needs to be said that it was quite surprising that low-inclined orbits do not seem to survive for long time. This, in a first sight, is contrary to the newly discovered Neptune Trojans which move almost in the same plane as Neptune. How come that we observe them? It can only be a transiting phenomenon that this objects stay for several million years there, and then escape. However, then there should exist a special process of capturing! But in a recent paper, Horner & Evans (2006) checked the possibility of

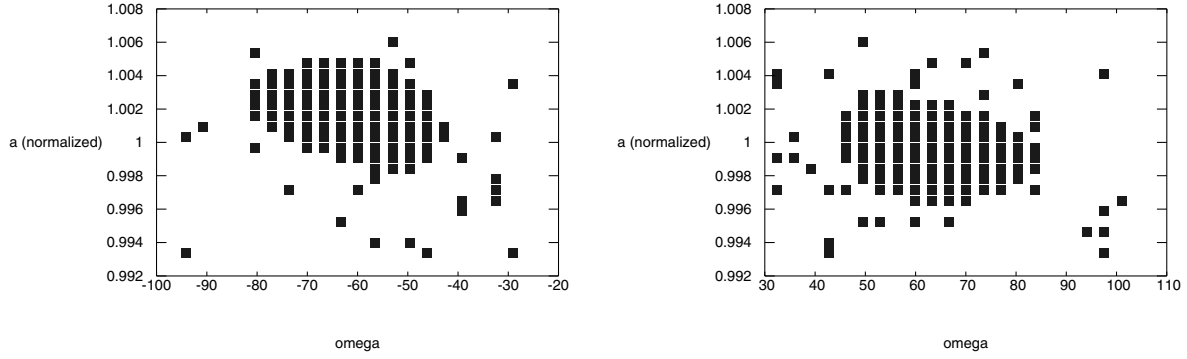


Figure 10. Stability regions around the Neptune equilateral equilibrium points L_5 (left-hand graph, located at $a = 1$ and -60°) and L_4 (right-hand graph, located at $a = 1$ and 60°) in model M8 for 10^7 yr.

captures of Centaurs into Trojan orbits; their results showed that Saturn is the most effective planet to capture Trojans and that Neptune in their computations could not capture even one Trojan out of more than 20 000 fictitious objects. As a consequence, we have no explanation for the existence.

Our results for the dynamics of the Neptune Trojans can be summarized as follows.

(i) No Trojans with low-inclined orbits survived for time-scales longer than 10^8 yr.

(ii) Most of the surviving orbits for the age of the Solar system were found with inclinations approximately $20^\circ \leq i \leq 40^\circ$.

(iii) There is a larger stable region around the following Lagrange point L_5 .

(iv) There exists a strong asymmetry between the two equilateral equilibrium points: whereas L_4 lies in the middle of the stability region $a - \omega$ L_5 is located almost outside the stable region which is shifted towards larger semimajor axes.

(v) This asymmetry, unique in the Solar system, is caused by Saturn and Uranus acting inside the Trojans' area of motion and is – most probably – due to secular resonances.

Nesvorný & Dones (2002) conjectured – in connection with the asymmetry of the stability areas for Neptune's Trojans – in their section 5.2 that 'this asymmetry should not be viewed as a signature of asymmetric long-term instabilities acting at Neptune's L_4 and L_5 points but rather originated from the choice of initial conditions'. In a footnote (p. 285), they stated that 'the asymmetry between the L_4 and L_5 Trojans is the largest for Neptune' and in addition that is due to Jupiter. However, in the paper by Holman & Wisdom (1993), from fig. 1 (p. 1992), it is concluded that only for Neptune this asymmetry is visible and not for Uranus. We did also computations for the Uranus' Trojans and could confirm these results (unpublished). The best argument in favour of real asymmetry is that in our model M8 there is no Jupiter and still it is present. Thus, we suspect the coupled influence of Saturn and Uranus to be the main cause for the asymmetry.

Nevertheless what needs to be investigated in future is the role of the different resonances acting in the zone of the Neptune Trojans,

similar to the complete study undertaken by Robutel et al. (2005) for the Jupiter Trojans. This work is in progress and will be published later.

ACKNOWLEDGMENTS

For the realization of this study, we need to thank the Austrian Science Foundation (FWF, project P16024-N05). RS did this work in the framework of a Schrödinger grant of the FWF (J2 619-N16); Thanks also go to the 'Wissenschaftlich-technische Zusammenarbeit Österreich-Ungarn' project A12-2004: Dynamics of extrasolar planetary Systems.

REFERENCES

- Celletti A., Giorgilli A., 1991, CeMDA, 50, 31
- Chambers J. E., 1999, MNRAS, 04, 793
- Chiang E. I., Lithwick Y., 2005, ApJ, 628, 520
- Dvorak R., Schwarz R., 2005, CeMDA, 92, 19
- Efthymiopoulos C., 2005, CeMDA, 92, 29
- Efthymiopoulos C., Sándor Z., 2005, MNRAS, 364, 253
- Érdi B., 1988, Celest. Mech., 43, 303
- Freistetter F., 2006, A&A, 453, 353
- Giorgilli A., Skokos Ch., 1997, A&A, 317, 254
- Hanslmeier A., Dvorak R., 1984, A&A, 132, 203
- Holman M. J., Wisdom J., 1993, AJ, 105, 1987
- Horner J., Evans N. W., 2006, MNRAS, 367, L20
- Lichtenegger H., 1984, Celest. Mech., 34, 357
- Marzari F., Tricarico P., Scholl H., 2003, A&A, 410, 725
- Nesvorný D., Dones L., 2002, Icarus, 160, 271
- Robutel P., Gabern F., Jorba A., 2005, CeMDA, 92, 53
- Schwarz R., Gyergyovits M., Dvorak R., 2004, CeMDA, 90, 139
- Sheppard S. S., Trujillo C. A., 2006, Sci, 313, 511
- Simó C., 1989, Mem. Real Acad. Ciencia y Artes de Barcelona, 48, 303
- Thommes E. W., Duncan M. J., Levison H. F., 1999, Nat, 435, 459
- Tsiganis M., Varvoglis H., Dvorak R., 2005, CeMDA, 92, 71.
- Zhou J. L., Sun Y. S., 2007, A&A, 464, 775

This paper has been typeset from a \LaTeX file prepared by the author.